PROGRESS IN AEROSPACE AND AVIATION TECHNOLOGY
e-ISSN: 2821-2924

PAAT

Vol. 5 No. 2 (2025) 30-41
https://publisher.uthm.edu.my/ojs/index.php/paat

Dynamic Modelling and System Identification of a Quadrotor Unmanned Aerial Vehicle Using Gyroscopic Based Test Stand

Haziqah Khudairi[1], Syariful Syafiq Shamsudin[1]*, Mohamad Fahmi Pairan[1], Nik Ahmad Ridhwan Nik Mohd[2], Mohd Shazlan Mohd Anwar[3]

[1] *Research Center for Unmanned Vehicles (RECUV), Faculty of Mechanical and Manufacturing Engineering, Universiti Tun Hussein Onn Malaysia (UTHM), Batu Pahat, 86400, MALAYSIA*
[2] *Aeronautics Research Center (UTM Aerolab), Faculty of Mechanical Engineering, Universiti Teknologi Malaysia, Skudai, 81310, MALAYSIA*
[3] *Virtual Instrument and System Innovation Sdn. Bhd. Petaling Jaya, 47301, MALAYSIA*

*Corresponding Author: syafiq@uthm.edu.my
DOI: https://doi.org/10.30880/paat.2025.05.02.004

Article Info

Received: 28 July 2025
Accepted: 16 November 2025
Available online: 31 December 2025

Keywords

System identification, test rig, state space modeling, quadrotor, unmanned aerial vehicles

Abstract

System identification plays a crucial role in developing accurate mathematical models for dynamic systems, which are essential for designing high-performance controllers. This study presents a novel gyroscope-based dynamic test rig developed specifically for quadrotor-type unmanned aerial vehicle (UAV) system identification. Unlike conventional outdoor testing, the proposed platform provides a controlled, repeatable, and vibration-minimized environment for capturing roll, pitch, and yaw dynamics, ensuring high data fidelity and safety. Using Mission Planner and LabVIEW grey box optimization, the research successfully identified continuous-time state space models that accurately characterize the UAV attitude behavior. The identified models achieved a mean squared error (MSE) below 0.002, indicating strong agreement between predicted and measured responses. These validated models formed the basis for tuning a PID controller, significantly enhancing flight stability and responsiveness. The proposed framework, which combines rig design, precise data acquisition, and data-driven modeling, provides a practical and scalable solution for UAV developers to perform pre-flight validation, reduce tuning time, and improve operational safety and control performance.

1. Introduction

Unmanned Aerial Vehicles (UAVs), particularly quadrotor drones, have gained prominence in applications such as agricultural monitoring, environmental surveillance, disaster management, and logistics due to their ability to perform autonomous maneuvers with high reliability [1], [2]. These vehicles exhibit nonlinear and coupled dynamics, which complicate the development of accurate mathematical models essential for controller design, safety, efficiency, and flight responsiveness. Traditional theoretical models often overlook real-world factors like aerodynamic effects, hardware imperfections, and environmental disturbances, leading to suboptimal performance in practical operations.

System identification, which derives mathematical models from measured input-output data, offers a data-driven alternative to address these limitations [3]. Notable contributions in this area include Tischler and Remple

[3], who established comprehensive frameworks for aircraft and rotorcraft system identification, emphasizing frequency-domain techniques for extracting dynamic parameters. Wei et al. [4] applied these methods specifically to quadrotors, identifying attitude dynamics and enabling flight control design through experimental data. Similarly, Liu and Chen [5] focused on modeling small unmanned helicopters, highlighting the importance of grey-box approaches for parameter estimation in under-actuated systems. Do et al. [6] validated quadrotor flight dynamics using simulation tools like X-Plane, comparing them with real flight data to assess model fidelity. Chipofya et al. [7] demonstrated trajectory tracking and stabilization using model predictive control based on identified dynamics, while Liu et al. [8] explored intelligent algorithms for UAV modeling and control, incorporating nonlinear elements.

Despite these advancements, gaps persist in the literature, including the lack of specialized test environments that provide controlled, repeatable conditions for quadrotor system identification without outdoor flight risks and limited integration of hardware like gyroscopic sensors with software tools for real-time parameter tuning [9], [10]. Conventional trial-and-error methods for controller adjustment remain inefficient, and many studies overlook cross-axis coupling in attitude dynamics, which can lead to instability. This study addresses these gaps by developing a gyroscopic-based test rig to facilitate accurate dynamic modeling and system identification of quadrotor UAVs. The approach involves designing a robust octagonal platform with a 6-degree-of-freedom gyroscope for measuring roll, pitch, and yaw rates; collecting flight data via Mission Planner under frequency-swept excitations; estimating state-space models using LabVIEW's grey-box optimization; and validating the models through residual analysis and mean squared error metrics. This methodology provides a structured framework for deriving aerodynamic coefficients, such as damping and control effectiveness, which will inform the discussion of results in terms of model accuracy and implications for PID controller tuning. In summary, the validated models from this work offer a foundation for enhancing UAV stability and responsiveness, with potential extensions to advanced controllers under varied conditions, contributing to safer and more efficient autonomous operations.

2. Methodology

The methodology for developing a dynamic test rig for system identification or PID tuning encompasses several important phases, beginning with the design and development of the test rig itself. This rig must be constructed to effectively simulate the desired system behaviors and should be equipped with essential sensors and actuators that facilitate the measurement and control of system parameters. The next phase involves system modeling, where a robust mathematical model is established to capture the dynamics and interactions of the system. This process includes data gathering through controlled experiments or simulations, followed by filtering to eliminate noise from the collected data. The gathered data is then utilized to train the model, which is subsequently validated to ensure its accuracy, with careful attention given to the appropriate sampling time to accurately capture the system dynamics.

2.1 Quadrotor Airframe and Instrumentation

The quadrotor airframe used in this project is based on a standard F450 FlameWheel ARF kit, which provides a stable and adaptable platform for testing and experimentation. The F450 platform is well suited to carrying a camera, brushless gimbal, small sensors, and a larger battery for longer flights. Pixhawk autopilots are a popular choice to be used for quadrotor projects due to their flexibility and advanced capabilities. The autopilots often include advanced sensors, such as the inertial measurement unit (IMU), barometers, and GPS, that provide the necessary data for flight stabilization and autonomous trajectory tracking. These sensors are critical for implementing system identification testing and control algorithms, ensuring stable flight. The system is synchronized with Mission Planner software, which generates excitation signals and logs actuator commands to ensure alignment between control inputs and measured outputs. Fig. 1 and Table 1 show the F450 quadrotor platform and the basic specification of the system.

Fig. 1 *The F450 quadrotor used for this project with the Pixhawk-based autopilot system*

Progress in Aerospace and Aviation Technology Vol. 5 No. 2 (2025) p. 30-41

Table 1 *The specification of the F450 quadrotor*

Frame	
Diagonal wheelbase	450 mm
Frame weight	282 g
Takeoff weight	800 - 1600 g
ESC	
Max allowable voltage	17.4 V
Max allowable peak current	30 A
Battery	3S–4S LiPo
Weight	27 g
Motor	
Stator size	23 × 12 mm
KV	960 rpm/V
Weight	57 g
Propeller	
Diameter/Pitch	24 × 12.7 cm
Weight (single)	13 g

2.2 Test Rig Design and Fabrication

The fabrication of the test rig is an essential component for analyzing flight dynamics, validating control systems, and conducting system identification in a controlled and repeatable environment. The rig consists of an octagonal aluminum platform supported by a mild steel frame, designed to provide structural stability and minimize vibration interference during dynamic tests. This configuration allows precise measurement of roll, pitch, and yaw motions by creating a controlled environment that closely replicates the rotational freedom experienced during actual UAV flights.

The test rig employs a 6-degree-of-freedom (DOF) gyroscope to capture angular velocity and orientation data, closely replicating actual UAV attitude dynamics under hover conditions. This setup offers unrestricted movement along all rotational axes, enabling comprehensive evaluation of UAV attitude dynamics while maintaining safety and containment. The user-friendly system architecture facilitates efficient iterations of controller tuning and testing, which markedly improve upon traditional trial-and-error methodologies.

Fig. 2 illustrates the comprehensive design framework of UAV test rigs employed for dynamic analysis and control system development. The test rig's robust design not only enhances the precision of dynamic measurements but also supports extended functions such as motor performance analysis under varying loads and real-time system response evaluations. Collectively, these features establish the rig as an effective platform for UAV control research and development, fostering improvements in stability and responsiveness essential for operational deployment.

(a) **(b)**

Fig. 2 *The test rig system prototype. (a) The structural design of the test rig system; (b) Quadrotor position in the test rig*

2.3 Kinematics and Dynamics Model of The Quadrotor UAV

Quadrotor-based UAS dynamics is known to be a non-linear model of a high-order multiple-input multiple-output (MIMO) system. It is also an under-actuated system with four actuator inputs: the thrust input $\boldsymbol{F}$, the rolling torque input produced by the forces of the right and left motors $\boldsymbol{\tau_\phi}$, the pitching torque input produced by the front and back motors $\boldsymbol{\tau_\theta}$ and the yawing torque input $\boldsymbol{\tau_\psi}$. The kinematics and dynamics of the quadrotor UAV can be described using Newton-Euler equations of motion and expressed by twelve-dimensional states. These state consists of quadrotor UAV position vectors in the inertial reference frame, $\boldsymbol{x}$, $\boldsymbol{y}$, and $\boldsymbol{z}$; the Euler angles (roll angle $\boldsymbol{\phi}$, pitch angle $\boldsymbol{\phi}$, and yaw angles $\boldsymbol{\psi}$); the quadrotor linear velocity in the body reference frame ($\boldsymbol{u}$, $\boldsymbol{v}$, and $\boldsymbol{w}$), and the quadrotor angular velocities in the body reference frame, ($\boldsymbol{p}$, $\boldsymbol{q}$, and $\boldsymbol{r}$). The motion of the quadrotor as expressed in the body reference frame is defined in Fig. 3.

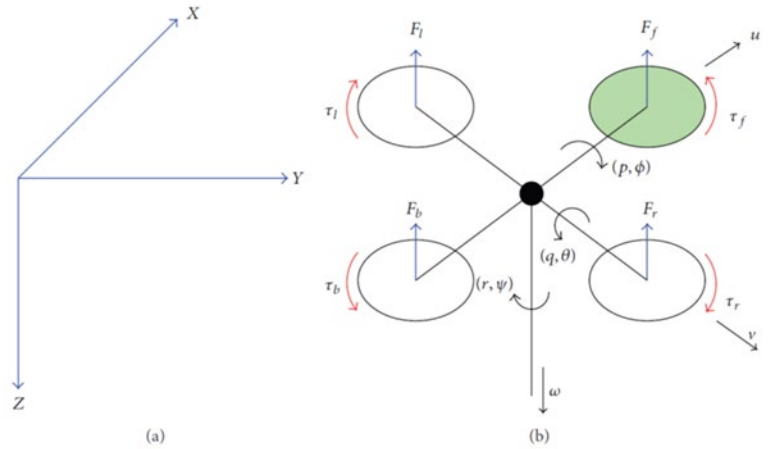

Fig. 3 *The free body diagram of a quadrotor UAV system [7]. (a) Inertial frame; (b) The forces and moments acting on the quadrotor body*

The overall dynamic of the quadrotor UAV can be divided into translational and rotational kinematics (Equations (1)-(2)) and translational and rotational dynamics (Equations (3)-(4)) as follows:

$$\begin{bmatrix}\dot{x}\\ \dot{y}\\ \dot{z}\end{bmatrix} = \begin{bmatrix}\cos\theta\cos\psi & \sin\phi\sin\theta\cos\psi - \cos\phi\sin\psi & \cos\phi\sin\theta\cos\psi + \sin\phi\sin\psi\\ \cos\theta\sin\psi & \sin\phi\sin\theta\sin\psi + \cos\phi\cos\psi & \cos\phi\sin\theta\sin\psi - \sin\phi\cos\psi\\ \sin\theta & -\sin\phi\cos\theta & -\cos\phi\cos\theta\end{bmatrix}\begin{bmatrix}u\\ v\\ w\end{bmatrix} \tag{1}$$

$$\begin{bmatrix}\dot{\phi}\\ \dot{\theta}\\ \dot{\psi}\end{bmatrix} = \begin{bmatrix}1 & 0 & tan\,\theta\,cos\,\phi\\ 0 & cos\,\phi & -sin\,\phi\\ 0 & \frac{sin\,\phi}{cos\,\theta} & \frac{cos\,\phi}{cos\,\theta}\end{bmatrix}\begin{bmatrix}p\\ q\\ r\end{bmatrix} \tag{2}$$

$$\begin{bmatrix}\dot{u}\\ \dot{v}\\ \dot{w}\end{bmatrix} = \begin{bmatrix}rv - qw\\ pw - ru\\ qu - pv\end{bmatrix} + \begin{bmatrix}-g\sin\theta\\ g\cos\theta\sin\phi\\ g\cos\theta\cos\phi\end{bmatrix} + \frac{1}{m}\begin{bmatrix}\Delta X\\ \Delta Y\\ \Delta Z\end{bmatrix} \tag{3}$$

$$\begin{bmatrix}\dot{p}\\ \dot{q}\\ \dot{r}\end{bmatrix} = \begin{bmatrix}\frac{I_{yy} - I_{zz}}{I_{xx}}qr\\ \frac{I_{zz} - I_{xx}}{I_{yy}}pr\\ \frac{I_{xx} - I_{yy}}{I_{zz}}pq\end{bmatrix} + \begin{bmatrix}\frac{1}{I_{xx}}\Delta L\\ \frac{1}{I_{yy}}\Delta M\\ \frac{1}{I_{zz}}\Delta N\end{bmatrix} \tag{4}$$

where $\boldsymbol{I_{xx}}$, $\boldsymbol{I_{yy}}$, and $\boldsymbol{I_{zz}}$ are the moments of inertia about body axes.

The nonlinear differential equation presented in Eq. (1)–(4) can be simplified into linear equations that can be used in linear controller design. If the roll angle $\boldsymbol{\phi}$, pitch angle $\boldsymbol{\theta}$ and yaw angle $\boldsymbol{\psi}$ are assumed to be operating in small angle ranges, the translational and rotational kinematic equations in Eq. (3) and (4) can be simplified as:

Progress in Aerospace and Aviation Technology Vol. 5 No. 2 (2025) p. 30-41

$$\begin{bmatrix} \Delta\dot{x} \\ \Delta\dot{y} \\ \Delta\dot{z} \end{bmatrix} = \begin{bmatrix} \Delta u \\ \Delta v \\ \Delta w \end{bmatrix} \tag{5}$$

$$\begin{bmatrix} \Delta\dot{\phi} \\ \Delta\dot{\theta} \\ \Delta\dot{\psi} \end{bmatrix} = \begin{bmatrix} \Delta p \\ \Delta q \\ \Delta r \end{bmatrix} \tag{6}$$

Similarly, the translational and rotational dynamics in Equations (3) and (4) can be further simplified if the roll angle, pitch angle, and the Coriolis terms, qr, pr, and pq are assumed to be small. Using the small perturbation approximation approach [3], the nonlinear equation of motion can be linearized as:

$$\begin{bmatrix} \Delta\dot{u} \\ \Delta\dot{v} \\ \Delta\dot{w} \end{bmatrix} = \begin{bmatrix} -g\Delta\theta + \dfrac{\Delta X}{m} \\ g\Delta\phi + \dfrac{\Delta Y}{m} \\ \Delta Z \end{bmatrix} \tag{7}$$

$$\begin{bmatrix} \Delta\dot{p} \\ \Delta\dot{q} \\ \Delta\dot{r} \end{bmatrix} = \begin{bmatrix} \dfrac{1}{I_{xx}}\Delta L \\ \dfrac{1}{I_{yy}}\Delta M \\ \dfrac{1}{I_{zz}}\Delta N \end{bmatrix} \tag{8}$$

The external forces $\boldsymbol{\Delta X}$, $\boldsymbol{\Delta Y}$ and $\boldsymbol{\Delta Z}$ and moments $\boldsymbol{\Delta L}$, $\boldsymbol{\Delta M}$ and $\boldsymbol{\Delta N}$ can be approximated as analytic function of disturbed motion variables and their derivatives during flight. The external forces and moments are presented as linearized perturbations as follows [4]:

$$\begin{bmatrix} \Delta X \\ \Delta Y \\ \Delta Z \\ \Delta L \\ \Delta M \\ \Delta N \end{bmatrix} = \begin{bmatrix} X_u u + X_q q + X_{\tau_\theta}\tau_\theta \\ Y_v v + Y_p p + Y_{\tau_\phi}\tau_\phi \\ Z_w w + Z_F F \\ L_v v + L_p p + L_{\tau_\phi}\tau_\phi + L_{\tau_\theta}\tau_\theta \\ M_u u + M_q q + M_{\tau_\phi}\tau_\phi + M_{\tau_\theta}\tau_\theta \\ N_r r + N_{\tau_\psi}\tau_\psi \end{bmatrix} \tag{9}$$

The linear state space model representing the quadrotor dynamics in hover flight can be derived as follows:

$$\begin{bmatrix} \dot{u} \\ \dot{v} \\ \dot{w} \\ \dot{p} \\ \dot{q} \\ \dot{r} \\ \dot{\phi} \\ \dot{\theta} \\ \dot{\psi} \end{bmatrix} = \begin{bmatrix} X_u & 0 & 0 & 0 & X_q & 0 & 0 & -g & 0 \\ 0 & Y_v & 0 & Y_p & 0 & 0 & g & 0 & 0 \\ 0 & 0 & Z_w & 0 & 0 & 0 & 0 & 0 & 0 \\ 0 & L_v & 0 & L_p & 0 & 0 & 0 & 0 & 0 \\ M_u & 0 & 0 & 0 & M_q & 0 & 0 & 0 & 0 \\ 0 & 0 & 0 & 0 & 0 & N_r & 0 & 0 & 0 \\ 0 & 0 & 0 & 1 & 0 & 0 & 0 & 0 & 0 \\ 0 & 0 & 0 & 0 & 1 & 0 & 0 & 0 & 0 \\ 0 & 0 & 0 & 0 & 0 & 1 & 0 & 0 & 0 \end{bmatrix} \begin{bmatrix} u \\ v \\ w \\ p \\ q \\ r \\ \phi \\ \theta \\ \psi \end{bmatrix} + \begin{bmatrix} 0 & 0 & X_{\tau_\theta} & 0 \\ 0 & Y_{\tau_\phi} & 0 & 0 \\ Z_F & 0 & 0 & 0 \\ 0 & L_{\tau_\phi} & L_{\tau_\theta} & 0 \\ 0 & M_{\tau_\phi} & M_{\tau_\theta} & 0 \\ 0 & 0 & 0 & N_{\tau_\psi} \\ 0 & 0 & 0 & 0 \\ 0 & 0 & 0 & 0 \\ 0 & 0 & 0 & 0 \end{bmatrix} \begin{bmatrix} F \\ \tau_\phi \\ \tau_\theta \\ \tau_\psi \end{bmatrix} \tag{10}$$

2.4 System Identification

The system identification process for the quadrotor UAV dynamics was conducted by utilizing input-output data gathered from a specially designed test rig equipped with a 6-DOF gyroscope and other sensors to capture precise real-time measurements of the UAV's roll, pitch, and yaw rates. The test rig's structurally stable and vibration-resistant platform ensured that the data collected were consistent and repeatable, which is crucial for accurate system modeling.

This work involves identifying the dynamic attitude of the quadrotor UAV through a system identification process. The measured input signals are the rolling torque input produced by the forces of the right and motors τ_ϕ, the pitching torque input produced by the front and back motors τ_θ and yawing torque input τ_ψ. The corresponding output angular rate responses, such as the angular velocities (p, q, and r) were also recorded establishing the necessary input-output relationship for analysis. The sampling frequency was set at 100 Hz, which is sufficiently higher than twice the maximum expected system frequency (based on the Nyquist criterion). This rate allows accurate capture of quadrotor dynamic responses up to 20 Hz, ensuring no loss of critical information.

Training and validation datasets use frequency-swept excitation to stimulate the system across frequencies. Example system dynamics excitation signals are shown in Fig. 4. System excitation must be adequate over the required frequency range. This range could potentially be 0.3–20 rad/s for quadrotor flight dynamics and control [6], [8]. Finally, a low-pass filter with a 10 Hz cut-off frequency was used to remove high-frequency noise in the data arising from structural vibration, sensor drift, and electrical interference.

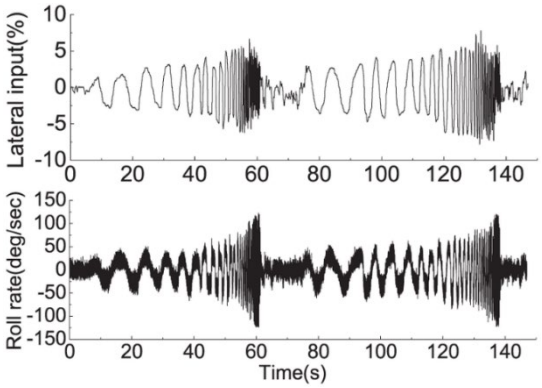

Fig. 4 *Example of frequency-swept data collected for lateral input and roll rate response [8]*

The corresponding input-output data were collected via Mission Planner during controlled flight tests of the quadrotor. To ensure consistency and robustness across the three axes (roll, pitch, and yaw), a standardized frequency sweep input was applied. The following parameters in Table 2 were configured for the excitation signals. These parameters define the characteristics of the excitation signals: (i) SID_MAGNITUDE controls the amplitude of the input excitation. (ii) SID_F_START_HZ and SID_F_STOP_HZ define the frequency sweep range, stimulating system dynamics from very low (0.05 Hz) to moderately high frequencies (5 Hz). (iii) SID_T_FADE_IN and SID_T_FADE_OUT ensure smooth transitions at the beginning and end of the excitation to reduce transients. (iv) SID_T_REC specifies the duration of each test sequence. In our implementation, the standard frequency sweeps (SID_AXIS 10, SID_AXIS 11, SID_AXIS 12) are used to directly add the frequency swept with the actuator inputs (τ_ϕ, τ_θ and τ_ψ). This systematic excitation and data acquisition process ensures that the collected data is suitable for developing accurate, high-fidelity dynamic models for each axis of motion [11].

Table 2 *The settings of the system identification model*

Mission Planner Configuration Parameters	Value		
	Roll Channel	Pitch Channel	Yaw Channel
SID_AXIS	10	11	12
SID_MAGNITUDE	0.15	0.15	0.55
SID_F_START_HZ	0.05 Hz	0.05 Hz	0.05 Hz
SID_F_STOP_HZ	5 Hz	5 Hz	5 Hz
SID_T_FADE_IN	5 s	5 s	5 s
SID_T_FADE_OUT	5 s	5 s	5 s
SID_T_REC	130 s	130 s	130 s

Using input-output data gathered from Mission Planner, two continuous-time state-space models were formulated to represent the attitude dynamics of the quadrotor [4], [5]:

The Coupled Roll-Pitch Dynamics:

$$\begin{bmatrix}\dot{\phi}\\ \dot{\theta}\\ \dot{p}\\ \dot{q}\end{bmatrix}=\begin{bmatrix}0 & 0 & 1 & 0\\ 0 & 0 & 0 & 1\\ 0 & 0 & L_p & 0\\ 0 & 0 & 0 & M_q\end{bmatrix}\begin{bmatrix}\phi\\ \theta\\ p\\ q\end{bmatrix}+\begin{bmatrix}0 & 0\\ 0 & 0\\ L_{\tau_\phi} & L_{\tau_\theta}\\ M_{\tau_\phi} & M_{\tau_\theta}\end{bmatrix}\begin{bmatrix}\tau_\phi\\ \tau_\theta\end{bmatrix}$$

Yaw Dynamics:

$$\begin{bmatrix}\dot{r}\\ \dot{\psi}\end{bmatrix}=\begin{bmatrix}N_r & 0\\ 1 & 0\end{bmatrix}\begin{bmatrix}r\\ \psi\end{bmatrix}+\begin{bmatrix}N_{\tau_\psi}\\ 0\end{bmatrix}\begin{bmatrix}\tau_\psi\end{bmatrix}$$

Parameter estimation was then performed using the 'SI Estimate Partially Known State-Space Model.vi' function in the LabVIEW Control Design and Simulation Module to estimate a state-space model for a partially known system from the input-output signals in the training dataset [12]. The function uses a grey-box estimation method that employs the Gauss-Newton optimization algorithm to minimize the mean squared error (MSE) between the estimated output of the model and the measured real output of the system. For grey-box models, which are systems with prior knowledge about the underlying dynamics or physical parameters, we can define constraints on certain parameters. These constraints can be set in two ways: (i) Setting constraint limits for the unknown parameter. The VI then randomly selects a value within this range as an initial guess and proceeds with optimization. Performing multiple estimates with a defined range can help increase the possibility of finding the global optimum. (ii) Setting Parameter Constraints with an Initial Guess: This initial guess, along with any specified upper and lower limits, serves as boundary constraints during the optimization process. The initial guess significantly influences the optimization's performance and whether it converges to a global or local optimum.

After estimation of the dynamic model parameters, the identified model was validated against separate data sets to ensure its generalization capability. This process involves comparing the model's output to actual system output data, utilizing a separate validation dataset that was not used during the model training phase. The quality of the model was evaluated using statistical metrics such as the mean squared error (MSE) and visual comparison of predicted versus actual responses.

This validated model provided a reliable foundation for further control system design, enabling the development and optimization of proportional-integral-derivative (PID) controllers and other advanced algorithms to enhance UAV stability, responsiveness, and operational safety under various flight conditions. Overall, this systematic, experimental-based approach to system identification significantly contributed to precise modeling of quadrotor dynamics, which is essential for advancing autonomous UAV control strategies and ensuring reliable flight performance.

3. Results and Discussion

This section discusses the outcomes from system identification processes and dynamic modeling, illustrating how the system identification models capture the quadrotor's behavior.

3.1 Parameter Estimation Results

Accurate estimation of the UAV's dynamic parameters is important when building reliable mathematical models and designing effective flight controllers. In this section, continuous-time state-space system identification techniques were employed to extract key aerodynamic and control parameters that characterize the quadrotor's attitude dynamics. Using flight data collected from the test rig, the LabVIEW Control Design module facilitated systematic optimization of model parameters by minimizing prediction errors.

The resulting parameter estimates provide insights into the UAV's inherent stability properties and control responsiveness. These parameters serve as empirical foundations for control system design, enabling precise tuning of algorithms such as PID controllers and facilitating simulation-based performance evaluation. Table 3 presents the parameter estimation result for the attitude dynamic model. Each parameter has a practical interpretation that directly informs UAV control system design, particularly for PID tuning and stability analysis. The damping coefficients (L_p, M_q, N_r) exhibit negative values, indicating their role as resistive effects that dissipate kinetic energy and enhance the UAV's inherent stability during angular rotations. The larger their magnitude, the more quickly the UAV returns to equilibrium after a perturbation. The control effectiveness parameters (L_{τ_ϕ}, M_{τ_θ}, N_{τ_ψ}) represent the sensitivity of the UAV's rotational rates to control inputs, determining

how effectively the vehicle's attitude responds to control commands. These control effectiveness gains describe how sensitive each rotational axis is to its respective control input. In practical terms, a higher control effectiveness value indicates that a smaller control effort is required to achieve a desired rate response, which allows the designer to assign a lower proportional gain (P-term) during PID tuning to maintain stability and prevent overshoot. Meanwhile, the cross-coupling gains (L_{τ_θ}, M_{τ_ϕ}) quantify the interactions between the roll and pitch axes, with significant coupling requires careful consideration in control system design to avoid unintended motions or instability. This necessitates careful tuning or use of decoupling strategies, especially for agile maneuvers.

Table 3 *Parameter estimation results*

Parameters	Description	Estimated Value	Practical Meaning	Control Design Implication
L_p	Roll damping	-7.5503	Higher magnitude produces a stronger damping effect, meaning the roll rate will decay faster after a disturbance.	A well-damped roll axis improves roll stability; PID derivative gain (D-term) can be tuned lower to avoid over-damping.
M_q	Pitch damping	-20.2831	Pitch oscillations are naturally attenuated more quickly.	Less aggressive derivative tuning is needed; controllers can prioritize responsiveness.
N_r	Yaw damping	-0.89142	Yaw oscillations persist longer and are harder to stabilize.	Requires a higher D-term or active damping through control feedback to improve yaw stability.
L_{τ_ϕ}	Lateral control effectiveness	-340.683	Large value means small input produces a strong roll response.	Roll control loop can use a smaller proportional gain (P-term) to avoid overshoot.
M_{τ_θ}	Longitudinal control effectiveness	-214.639	Strong but slightly weaker than the roll axis, consistent with structural symmetry.	Pitch control gain can be set proportionally lower than roll.
N_{τ_ψ}	Yaw control gain	52.1082	Positive value indicates direct and stable yaw response.	Used to scale yaw control inputs for consistent rotational behavior.
L_{τ_θ}	Roll-to-pitch coupling	-85.7437	Cross-axis interference exists and affects stability if not compensated.	The controller must include decoupling terms or use a multi-input design (e.g., state feedback, or MPC).
M_{τ_ϕ}	Pitch-to-roll coupling	360.087	Significant asymmetry: pitch maneuvers influence roll dynamics.	Suggests need for coupled controller design, or at minimum, reduced P-gain in roll when pitch commands are active.

Several approaches have been demonstrated in the literature, where identified aerodynamic derivatives and control effectiveness parameters were employed to guide PID tuning for small-scale UAVs and rotorcraft systems, such as in the studies by Tischler and Remple [3], Wei et al. [4], and Liu and Chen [5], who showed that incorporating these stability derivatives into the controller design significantly improves attitude tracking performance and transient response behavior. Building upon these findings, the parameters identified in this work provide a solid foundation for model-based PID controller design, where gain values can be systematically derived from dynamic response characteristics rather than relying solely on heuristic trial-and-error methods [13], [14], [15]. Furthermore, they open opportunities for adaptive or gain-scheduled PID strategies, where controller parameters are adjusted in real time based on variations in damping or control effectiveness values across different flight regimes. This integration of system identification with data-informed control tuning represents a key step toward achieving high-performance, robust, and energy-efficient flight control for quadrotor UAVs.

The training graphs illustrate the comparison between the predicted outputs produced by the identified state-space models and the actual sensor data recorded during flight tests for roll rate (p), pitch rate (q), and yaw rate (r). The Mean Squared Error (MSE) metric was used to measure the difference between the model's predicted

Progress in Aerospace and Aviation Technology Vol. 5 No. 2 (2025) p. 30-41

outputs and the actual sensor measurements. This is an objective way to measure how well the model fits. Lower MSE values indicate a closer alignment between predicted and measured signals, thereby demonstrating the model's ability to accurately reproduce the UAV's dynamics during flight. Fig. 5 shows the roll rate, pitch rate, and yaw rate prediction response for the quadrotor UAV. The predicted roll rate follows the data measured closely during the training interval, indicating effective capture of the roll axis dynamics. The training MSE for roll was 0.10240, reflecting a good fit despite the complexity and possible disturbances on this axis. The pitch rate model accurately matched the recorded pitch measurements with a training MSE of 0.06807, signifying a slightly better fit than the roll axis, potentially due to less noise or coupling effects. The yaw dynamics were modeled with the lowest training MSE of 0.0034, showing a near-perfect fit between predicted and actual yaw rate data. This suggests the yaw behavior was relatively consistent and well-suited to the chosen modeling approach.

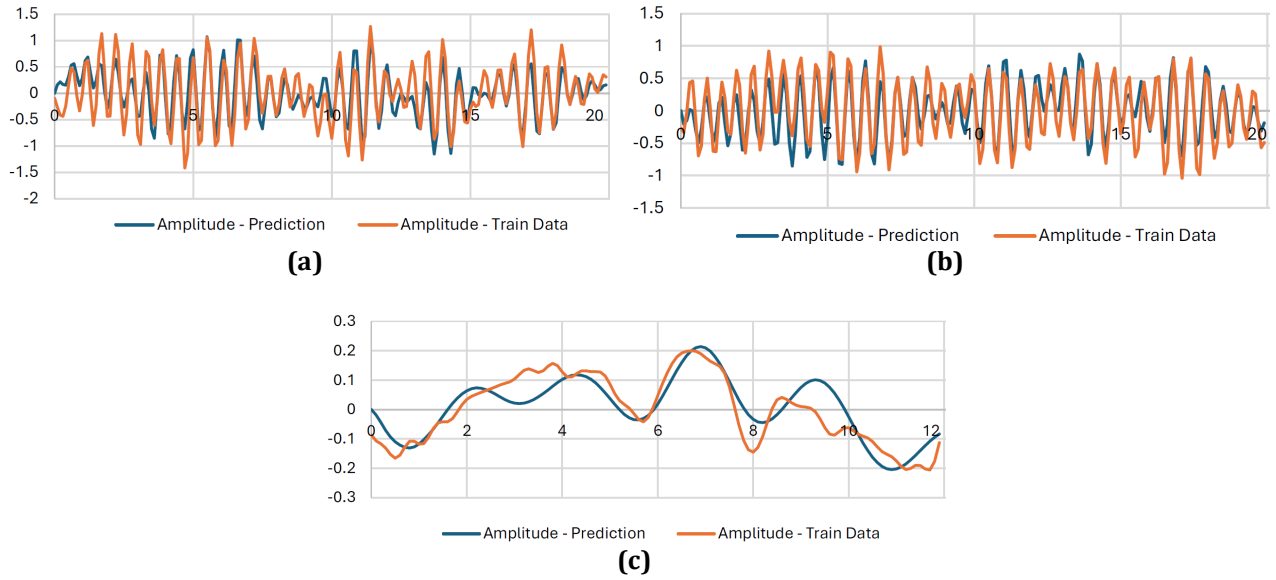

Fig. 5 *Model prediction performance vs. training data. (a) Roll rate prediction; (b) Pitch rate prediction; and (c) Yaw rate prediction*

The training phase of the state-space model estimation demonstrated promising results, reflected by the relatively low Mean Squared Error (MSE) values obtained for the roll, pitch, and yaw dynamics. These results indicate that the grey box estimation model approach effectively modeled the responses of the UAV with the training dataset. The lower MSE value for yaw compared to roll and pitch suggests that the yaw dynamics exhibited more consistent or less noisy patterns during experimentation, which facilitated a better fit for the model. Meanwhile, the higher MSE for roll dynamics may be due to the increased complexity or disturbances affecting that axis, such as cross-coupling effects or sensor noise. Nonetheless, the MSE values remain within acceptable limits, confirming the suitability of the identified models for further validation and control design purposes. It is important to note that the training segment was carefully chosen from flight data rich in dynamic activity to ensure the model could learn the UAV's behavior comprehensively. However, training on limited or overly specific data segments might risk overfitting. Subsequent validation stages are therefore crucial to verifying the model's capacity to generalize outside of the training environment. Overall, the training configuration combining partially known state-space modeling and systematic parameter optimization has established a reliable mathematical representation of the UAV's attitude dynamics. These models provide a solid foundation for developing advanced control strategies, such as PID tuning or adaptive control, which ultimately contribute to improved UAV stability and responsiveness in real-world flight scenarios.

3.2 Model Validation

Following the identification of the state-space dynamic models for the quadrotor UAV's roll, pitch, and yaw dynamics, rigorous model validation is essential to ensure the models accurately capture the real system behavior and generalize well to new, unseen data. Model validation involves comparing the predicted outputs of the identified models against separate experimental datasets that were not involved in the training phase. This process assesses the model's predictive performance, robustness, and suitability for real-time control applications. The validation metrics, primarily the mean squared error (MSE), serve as quantitative indicators of discrepancy between model outputs and actual sensor measurements, with lower MSE values indicating better model fidelity.

Residual analysis and statistical consistency checks further confirm that the identified models do not overfit training data and reliably replicate the UAV's dynamic response across all three rotational axes. The validated models provide a trustworthy foundation for subsequent control design, including tuning of Proportional-Integral-Derivative (PID) controllers, to improve the stability and responsiveness of the UAV in practical operations. Fig. 6 presents the comparison between the actual measured data from the UAV sensors and the predicted outputs (*p, q*, and *r*) generated by the identified state-space models during validation. Fig. 5(a) plots the amplitude of the predicted roll rate against the actual measured values over a validation data segment. The close overlap of predicted and measured signals indicates that the model accurately tracks the roll dynamics with minimal error, confirmed by a validation MSE of approximately 0.0814. Similarly, the plot of pitch rate validation in Fig. 6(b) shows the predicted model output matches closely the measured sensor data during the validation phase. The MSE of about 0.111 reflects slight deviations yet remains within acceptable bounds, indicating reliable model generalization. For the yaw rate prediction in Fig. 6(c), the predicted output and measured data exhibit adequate prediction performance, with an increase in MSE of 0.0238 compared to the MSE in prediction using the training dataset. The prediction accuracy for the identified yaw dynamic model can be further improved by using a coupled attitude model with more stability derivatives, as suggested in [7] and [16], to satisfactorily represent the yaw dynamic. Overall, the relatively low error signifies excellent predictive accuracy and robustness, demonstrating the model's capability to effectively replicate the UAV's yaw behavior in a new dataset. These validation results collectively affirm that the models developed from the experimental data provide a true representation of the quadrotor's dynamic behavior, ensuring high confidence for use in designing and optimizing flight controllers.

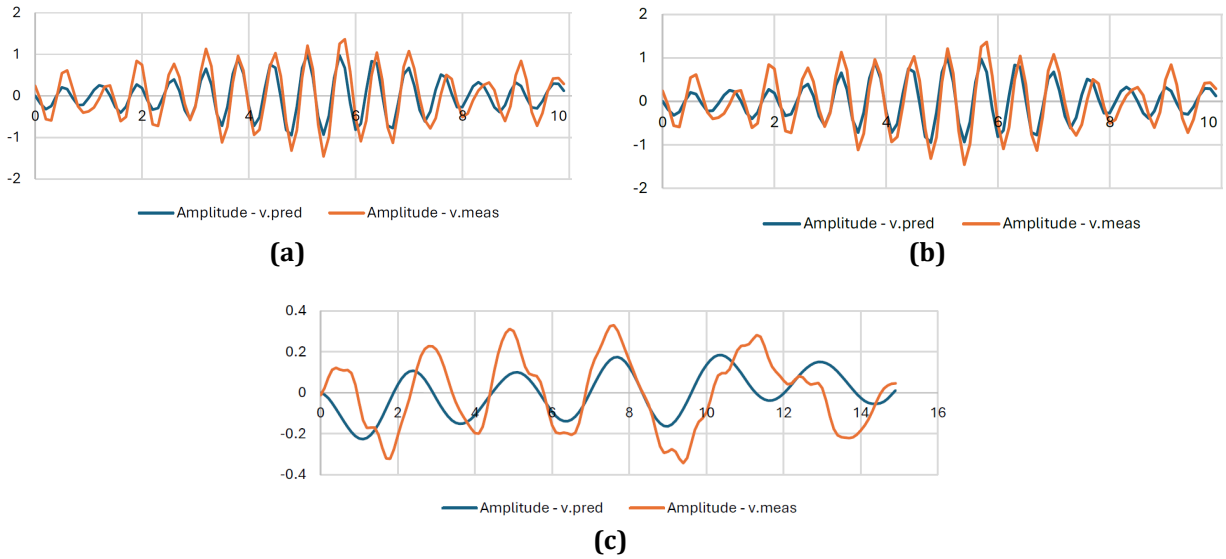

Fig. 6 *Model prediction performance vs. validation data. (a) Roll rate prediction; (b) Pitch rate prediction; and (c) Yaw rate prediction*

4. Conclusion

This study successfully developed and implemented a gyroscope-based dynamic test rig designed to facilitate accurate system identification and dynamic modeling of a quadrotor UAV under controlled laboratory conditions. The test rig's rigid structure and the addition of a six-degree-of-freedom gyroscope made it possible to gather high-quality input-output data for estimating continuous-time state space models. The identified models demonstrated strong agreement with measured responses, as indicated by low mean squared error (MSE) values across roll, pitch, and yaw dynamics. These results confirm the capability of the proposed test environment and modeling framework to capture key aerodynamic and control characteristics of the UAV, thereby providing a reliable basis for PID controller design and performance optimization.

Despite these encouraging outcomes, several limitations should be acknowledged. First, experimental validation was conducted exclusively in an indoor, controlled environment, which may not fully replicate real-world flight conditions where external disturbances such as wind gusts, aerodynamic coupling, and environmental noise play significant roles. Second, the identified models primarily represent linearized dynamics around hover flight, limiting their applicability under aggressive maneuvers or high-angle attitudes where nonlinear effects become dominant. Third, the current test rig does not incorporate multi-sensor fusion (e.g., vision-based feedback or GPS data), which could enhance state estimation accuracy during extended or autonomous flight tests.

Future research should address these limitations by extending the system identification framework to outdoor or semi-open environments, enabling validation under realistic operational conditions and disturbance profiles. Incorporating nonlinear modeling techniques, such as neural network-based system identification or physics-informed models, can improve prediction accuracy across a broader flight envelope. Moreover, integrating adaptive and gain-scheduled control algorithms that leverage the identified stability derivatives will enhance robustness against environmental variations and payload changes. Finally, expanding the test rig's capabilities to include hardware-in-the-loop simulations, multi-axis force-torque sensing, and real-time flight testing will further advance its utility as a comprehensive platform for UAV modeling, control development, and validation. In summary, the present work demonstrates a robust and systematic approach to UAV dynamic modeling using a gyroscope-based test stand. With future refinements to address environmental realism, nonlinearities, and adaptive control integration, the proposed framework can significantly contribute to the development of safer, more stable, and higher-performing autonomous aerial systems.

Acknowledgement

This research was supported by Universiti Tun Hussein Onn Malaysia (UTHM) through Tier 1 (Vot. Q898) research grant.

Conflict of Interest

Authors declare that there is no conflict of interest regarding the publication of the paper.

Author Contribution

The authors confirm their contribution to the paper as follows: ***study conception and design:*** *Haziqah Khudairi and Syariful Syafiq Shamsudin;* ***data collection:*** *Mohamad Fahmi Pairan and Haziqah Khudairi****; analysis and interpretation of results:*** *Mohamad Fahmi Pairan, Haziqah Khudairi, and Syariful Syafiq Shamsudin;* ***draft manuscript preparation:*** *Haziqah Khudairi, Syariful Syafiq Shamsudin, Nik Ahmad Ridhwan Nik Mohd, and Mohd Shazlan Mohd Anwar. All authors reviewed the results and approved the final version of the manuscript.*

References

[1] R. S. Geronel, R. M. Botez, and D. D. Bueno, "Dynamic responses due to the Dryden gust of an autonomous quadrotor UAV carrying a payload," *The Aeronautical Journal*, vol. 127, no. 1307, pp. 116–138, Jan. 2023, doi: 10.1017/aer.2022.35.

[2] T. Karachalios, P. Moschos, and T. Orphanoudakis, "Maritime Emission Monitoring: Development and Testing of a UAV-Based Real-Time Wind Sensing Mission Planner Module," *Sensors*, vol. 24, no. 3, p. 950, Feb. 2024, doi: 10.3390/s24030950.

[3] M. B. Tischler and R. K. Remple, *Aircraft and Rotorcraft System Identification, Second Edition*. 2012. doi: 10.2514/4.868207.

[4] W. Wei, M. B. Tischler, N. Schwartz, and K. Cohen, "System Identification and Flight Control of an Unmanned Quadrotor," in *Advanced UAV Aerodynamics, Flight Stability and Control*, Wiley, 2017, pp. 695–727. doi: 10.1002/9781118928691.ch21.

[5] C. Liu and W. Chen, "Dynamics Modelling and System Identification of Small Unmanned Helicopters," in *Advanced UAV Aerodynamics, Flight Stability and Control*, Wiley, 2017, pp. 255–282. doi: 10.1002/9781118928691.ch7.

[6] M.-H. Do, C.-E. Lin, and Y.-C. Lai, "Validation of the Flight Dynamics Engine of the X-Plane Simulator in Comparison with the Real Flight Data of the Quadrotor UAV Using CIFER," *Drones*, vol. 7, no. 9, p. 548, Aug. 2023, doi: 10.3390/drones7090548.

[7] M. Chipofya, D. J. Lee, and K. T. Chong, "Trajectory Tracking and Stabilization of a Quadrotor Using Model Predictive Control of Laguerre Functions," *Abstract and Applied Analysis*, vol. 2015, pp. 1–11, 2015, doi: 10.1155/2015/916864.

[8] P. Liu, X. Luo, Z. Bai, X. Liu, and J. Liu, "Research on unmanned aerial vehicle modeling and control based on intelligent algorithms," *Advances in Mechanical Engineering*, vol. 11, no. 5, May 2019, doi: 10.1177/1687814019851693.

[9] A. Brezina and S. Thomas, "Measurement of Static and Dynamic Performance Characteristics of Electric Propulsion Systems," in *51st AIAA Aerospace Sciences Meeting including the New Horizons Forum and Aerospace Exposition*, Reston, Virigina: American Institute of Aeronautics and Astronautics, Jan. 2013. doi: 10.2514/6.2013-500.

[10] S. A. Araujo-Estrada, M. H. Lowenberg, S. Neild, and M. Goman, "Evaluation of Aircraft Model Upset Behaviour Using Wind Tunnel Manoeuvre Rig," in *AIAA Atmospheric Flight Mechanics Conference*, Reston, Virginia: American Institute of Aeronautics and Astronautics, Jan. 2015. doi: 10.2514/6.2015-0750.

[11] ArduPilot Dev Team, "System ID Mode Operation." Accessed: Jul. 25, 2025. [Online]. Available: https://ardupilot.org/copter/docs/systemid-mode-operation.html

[12] National Instruments, "LabVIEW System Identification Toolkit User Manual," Austin, Texas, Sep. 2004. Accessed: Jul. 28, 2025. [Online]. Available: https://download.ni.com/pub/gdc/tut/usermanual.pdf

[13] L. Wang, *PID Control System Design and Automatic Tuning using MATLAB/Simulink*. Wiley, 2020. doi: 10.1002/9781119469414.

[14] S. H. Yi, S. S. Shamsudin, and M. F. Pairan, "Flight Control System Design for a Rotorcraft-Based Unmanned Aerial System using Pole Placement and LQR-Based PID Tuning Techniques," *Journal of Aeronautics, Astronautics and Aviation*, vol. 56, no. 3, pp. 615–636, 2024, doi: 10.6125/JoAAA.202407_56(3).01.

[15] A. S. Jemsa, S. S. Shamsudin, and M. F. Pairan, "Flight Control System Design and Dynamic Simulation for DJI F450 Quadcopter UAV Using Pole Placement Tuning Method," *Progress in Aerospace and Aviation Technology*, vol. 4, no. 2, pp. 17–35, Dec. 2024, doi: 10.30880/paat.2024.04.02.003.